Orbital Specificity in the Unoccupied States of UO_2 from Resonant Inverse Photoelectron Spectroscopy

J. G. Tobin* and S.-W. Yu

Lawrence Livermore National Laboratory, Livermore, California, USA 94550

(Received 4 May 2011; published 14 October 2011)

One of the crucial questions of all actinide electronic structure determinations is the issue of 5f versus 6d character and the distribution of these components across the density of states. Here, a breakthough experiment is discussed, which has allowed the direct determination of the U5f and U6d contributions to the unoccupied density of states in uranium dioxide. A novel resonant inverse photoelectron and x-ray emission spectroscopy investigation of UO_2 is presented. It is shown that the U5f and U6d components are isolated and identified unambiguously.

DOI: 10.1103/PhysRevLett.107.167406 PACS numbers: 78.70.En, 71.20.Gj, 71.20.Ps, 78.70.Dm

Uranium dioxide is the most widely used nuclear fuel for the generation of electrical power [1,2]. Because of the important role that computational simulations play in the pursuit of safety within nuclear power generation, a detailed knowledge of the electronic structure of uranium dioxide is crucial for the benchmarking of these models and theories [2]. Hence, it is not surprising that uranium and uranium dioxide have been widely studied for many decades with an immense variety of theoretical models and electron spectroscopic techniques [3]. An incomplete sampling of the experimental studies includes ultraviolet and x-ray Photoelectron spectroscopy (UPS and XPS) [4–10], bremsstrahlung isochromat spectroscopy (BIS) [5], inverse photoelectron spectroscopy (IPES) [11,12], electron energy loss spectroscopy [8], x-ray absorption spectroscopy (XAS) [13–16], resonant photoelectron spectroscopy [17], and resonant inverse photoelectron spectroscopy (RIPES) [18]. Recent theoretical treatments have emphasized both the ionic nature [19] and covalency [20] in uranium dioxide.

A common thread through the studies of the core levels, particularly those using photoelectron spectroscopy [4–10], has been the observation of satellite structure in uranium dioxide. For example, there is strong and unique satellite structure in the U4d and U4f spectra of uranium dioxide. [5,6,8,10] The observation and analysis of satellite structure in general has an extensive and distinguished history [21,22]. Carlson and co-workers made some of the earliest reports [23,24], and there has long been evidence that the satellite structure can, in fact, be larger than the nominal "main" features [22,25]. In the case of UO_2, satellites are seen with a variety of spectroscopies. However, they are observed at all kinds of different energies and different intensities, suggesting different origins. For example, Allen *et al.* in Ref. [6] have the following results: the U4f XPS satellites are separate features at about 7 eV and 16 eV; the U4d PES satellites are each just a shoulder on the main peak; the U5p3/2 satellite is at 17 eV; the U5d satellite is about 8 eV from the main peak. In Ref. [5], Baer and Schoenes report a satellite in the U4f spectra at 7 eV and there is evidence in their data of another satellite at higher energies. The XAS satellites, reported by Kalkowski *et al.* in Fig 5 in Ref. [13], are very weak and about 20 eV away from the main feature. It seems unlikely that a single effect can explain all of these observations. Now, we present evidence of novel satellites in the resonant IPES of UO_2, at yet again a different energy.

Here, the first observation of such satellite structure in the RIPES and x-ray emission spectroscopy (XES) of UO_2 is reported (Figure 1). Superficially, IPES, RIPES and XES look the same. There is an incoming monoenergetic beam

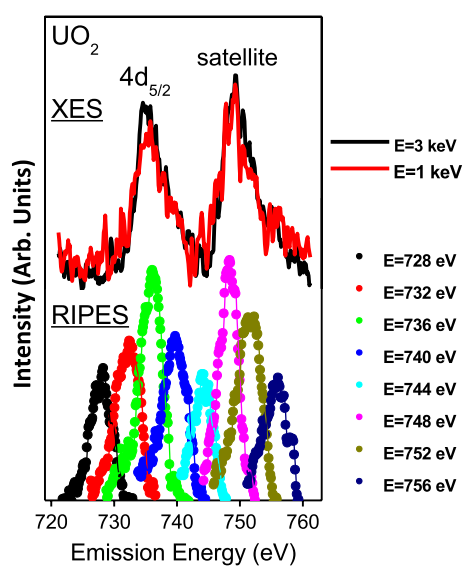

FIG. 1 (color online). The RIPES and XES of UO_2 is presented here. The XES is shown in the upper part of the figure and the RIPES in the lower part of the figure. Backgrounds have been subtracted. The legend denotes the energy of the excitation, i.e., the incoming electrons. The horizontal scale on the bottom is the energy of the outgoing photons. The resolution bandpass was 2 eV or better throughout, as described in Ref. [26]. Note that the satellite is as large as the main peak. See text for details.

 © 2011 American Physical Society

of electrons used as the excitation and the emitted photons are energy selected using a monochromator and then detected using channel plate technology. However, there are significant differences between each. In XES, the beam of electrons is chosen to be of a fairly high energy, substantially above the energy of the core levels that are to be vacated. The photons emitted are produced in the decay process to fill these holes and thus have energies corresponding to the core levels. In IPES, a very different set of circumstances prevails. Here, the energies of the incoming electrons and emitted photons are roughly the same. The electrons drop down and fill the low-lying unoccupied states, giving a measure of the unoccupied density of states (UDOS) just above the Fermi level or band gap. RIPES is, in a sense, a combination of the conditions of XES and IPES: the incoming electrons, the emitted photons and the core level electrons all are roughly equivalent. Thus, two channels are now available: the direct channel as in IPES and the indirect channel through the core level, as in XES. The ramifications of all of this will be discussed in more detail below.

It should be noted, that the resonant variants of photoelectron spectroscopy and inverse photoelectron spectroscopy can be viewed as manifestations of the wave interference effects that are commonly referred to as "Young's two slit problem." Thus, because of the unique constraints placed upon RIPES owing to its quantum-mechanical nature [26,27] and the availability of a recently verified model of the complex internal structure of the UDOS of uranium dioxide involving both U5f and U6d states [16], it will be shown that the main and satellite peaks in the RIPES correspond to the 5f and 6d thresholds of the unoccupied DOS. This result opens the door to application of this approach to the more radioactive actinides and the isolation of their 5f and 6d components in the UDOS.

The experiments were performed on site at Lawrence Livermore National Laboratory, using a spectrometer configured to perform spin resolved photoelectron spectroscopy and inverse photoelectron spectroscopy [10,26,28]. The preparation of the UO_2 sample is described in detail elsewhere, including an exhaustive characterization with XPS and UPS *in situ* [10]. The high quality of the origin and history of the underlying uranium substrate has been demonstrated previously [7,10]. The technical specifics of the RIPES and XES measurements, such as the monochromator calibration and resolution determination, have been discussed earlier in a study of Ce oxide [26]. The methodology of the supporting XAS study has also been reported in a prior publication [16].

Before beginning the discussion and interpretation of the RIPES and XES results, it is useful to digress to a consideration of the structure of the UDOS in UO_2. Recently, along with several collaborators, we reported on a determination of the UDOS of the uranium dioxide system, using XAS, bremsstrahlung isochromat spectroscopy (BIS, also known as high energy Inverse Photoelectron Spectroscopy, IPES) and XPS [16]. A summary of our experimental results is shown in Fig. 2. The result of these measurements is that it is shown that the UDOS of UO_2 is composed principally of two sectors: one dominated by U5f and O2p contributions and the other by U6d and O2p contributions. These are shown schematically in Fig. 2 as a green band (U5f and O2p) and a red band (U6d and O2p). Underlying this analysis is the well-founded assumption that these XAS soft x-ray transitions will be driven by electric dipole matrix elements, with Δl equaling $+/-$ 1. Thus, the transition from the U4f core state gives us a measure of the UDOS associated with the U6d ($\Delta l = -1$), the U4d transition gives us a measure of the UDOS associated with the U5f ($\Delta l = 1$) and the O1s transition gives us a measure of the UDOS associated with the O2p states ($\Delta l = 1$). This is further confirmed by the BIS result, which shows a large peak over the U5f region, but minimal intensity in the U6d area. Our observations of BIS at 915 eV are in strong agreement with that reported, many years earlier, at a higher energy, by Baer and Schoenes [5]. This selectivity of the BIS for the U5f over the U6d is a cross-sectional effect. As shown by Yeh and Lindau [29] for photoelectron spectroscopy, the U5f cross sections at these energies are an order of magnitude larger than the cross sections of the U6d. Because, in some limited sense, IPES can be thought of in terms of a time reversal of photoelectron spectroscopy, the matrix elements are the same but the results must be corrected for initial and final state densities. Performing these functions, the result is obtained that the U5f should dominate the U6d transitions in BIS. However, it should be noted that at the lowest energies, there is the possibility that the U6d in

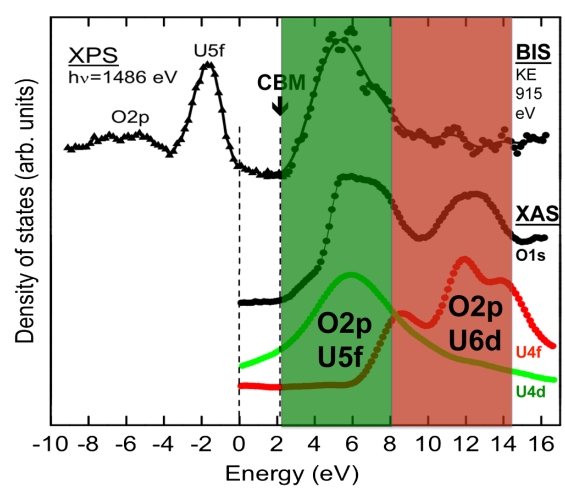

FIG. 2 (color online). A summary of our earlier results for XPS, BIS and XAS of UO_2 is shown here. The green region represents the part of the UDOS dominated by U5f and O2p states and the red area is that dominated by the U6d and O2p states. See text for details. CBM is conduction band minimum, as defined and utilized in Ref. [16].

IPES may be seen. That is indeed the case: Chauvet and Baptist observed a small, broad feature in the U6d region using IPES, particularly at the lowest energy ($\lambda = 600$ angstroms, hv of about 21 eV) [3,11]. Although the U6d cross sections may surpass the U5f cross sections in this regime [29], observation of a strong U6d feature may be hindered by the broad distribution of states implied by the results in Fig. 2. (The U6d XAS broadening is derived from the state distribution, while the U5f peaks have more lifetime (XAS) and instrumental (BIS) contributions [16].) Furthermore, the experimental picture of the distribution of U5f, U6d and O2p states in the UDOS is supported by the calculations in our earlier paper [16] and those of others [20]. It is within this picture of the UDOS in UO_2 that the RIPES and XES of UO_2 will be discussed and explained. In fact, this picture is essential to an analysis of the new RIPES results for UO_2. However, it should be noted that soft x-ray absorption experiments, such as that discussed above, are possible upon unencapsulated samples at synchrotron radiation facilities only if the actinide has low radioactivity. Thus, there is a need for a technique with equivalent capabilities, which can be performed in house, for application to the more radioactive members of the actinides. It is shown here that RIPES can satisfy that need.

The XES and RIPES results for uranium dioxide are plotted in Fig. 1. It should be noted that these data are intrinsically cross-calibrated. For each of the spectra, the detector energy position is the same. The data collection is performed by wavelength selection with a grating monochromator and then the photons are counted with multichannel detection. In these measurements, the energy position of the monochromator and center of the channel plate are each fixed and the different photon energies are dispersed across the channel plate. The only parameter varied is the kinetic energy (KE) of the incoming electron.

At high kinetic energies, e.g., 1 keV and 3 keV, the result is core hole generation and photon emission due to the filling of the core hole. Thus, the XES tends to be associated with a specific core level. In this case, the core level is the U4$d_{5/2}$. This can all be summarized in Eq. (1).

$$e(\mathrm{KE}^{\mathrm{XES}}) + (4d_{5/2})^6(\mathrm{VB} - 5f)^2 \rightarrow (4d_{5/2})^5(\mathrm{VB} - 5f)^2 + 2e \quad (1a)$$

$$(4d_{5/2})^5(\mathrm{VB} - 5f)^2 \rightarrow (4d_{5/2})^6(\mathrm{VB} - 5f)^1 + \mathrm{hv}^{\mathrm{XES}} \quad (1b)$$

$$\mathrm{hv}^{\mathrm{XES}} \approx \mathrm{BE}(4d_{5/2}) \quad (1c)$$

VB stands for valence band and hv is the photon energy. This is, in fact, what is observed for the first XES peak near a photon energy of 735 eV, which is close to the binding energy (BE) of the U4$d_{5/2}$ level, 740 eV relative to the valence band maximum, or 742 eV relative to the conduction band minimum (CBM) [4,10]. There is another intense peak in the XES spectrum near a photon energy of 749 eV. This peak cannot be the 4$d_{3/2}$ feature: although not shown here, we observe another peak at a photon energy of about 780 eV, which gives the correct spin-orbit splitting for the $5/2 - 3/2$ 4d doublet, agreeing with our earlier XPS data [10]. However, to explain the observation of such a strong peak at 749 eV will require a discussion of the RIPES. Next, we discuss the origin of the peak at 749 eV.

The IPES results, both slightly off resonance (BIS/IPES) and directly on resonance (RIPES), are shown in the bottom of Fig. 1. There is a linear relationship between the kinetic energy of the incoming electron and the emitted photon: this can be seen in the dispersion of the IPES peak with the excitation energy. The relationships are shown in Eq. (2).

$$e(\mathrm{KE}^{\mathrm{IPES}}) + (4d_{5/2})^6(\mathrm{VB} - 5f)^2 \rightarrow (4d_{5/2})^6(\mathrm{VB} - 5f)^2(\mathrm{CB} - 5f)^1 + \mathrm{hv}^{\mathrm{IPES}} \quad (2a)$$

$$\mathrm{hv}^{\mathrm{IPES}} \approx \mathrm{KE}^{\mathrm{IPES}} \quad (2b)$$

CB stands for conduction band. Before going on to a discussion of RIPES, two aspects of IPES should be noted. First, the IPES peak, which reflects the unoccupied density of 5f states with instrumental broadening, is much sharper than the XES peaks. This observation for uranium dioxide is consistent with our earlier work on RIPES in cerium oxide [26]. Second, by measuring the IPES of UO_2 over a wide range, hv = 720–915 eV, a quantitative, absolute calibration of the energy scale of the photon detection monochromator was performed [26]. An example of that IPES data is shown in Fig. 2.

At the energy corresponding to the U4$d_{5/2}$ level, the nature of IPES changes. Here a resonance can occur, where the kinetic energy of the incoming electron just matches the binding energy of the core level. Under these conditions, a second (indirect) channel can open up. However, both channels, direct and indirect, must end at the same electronic configuration. A summary of these relationships is shown in Eq. (3) and illustrated schematically in the left panels of Fig. 3. (Please note that the scheme for XES would be similar to the indirect channels in Fig. 3, except that neither the incoming excitation electron nor the excited core electron would reside in the bound unoccupied density of states. See Ref. [26] for more detail.)

$$\begin{array}{lcl} & \text{Direct} & \\ e(\mathrm{KE}^{\mathrm{RIPES}}) + (4d_{5/2})^6(\mathrm{VB\text{-}5f})^2 & \rightarrow & (4d_{5/2})^6(\mathrm{VB\text{-}5f})^2(\mathrm{CB\text{-}5f})^1 + \mathrm{hv}^{\mathrm{RIPES}} \\ \text{Indirect} \quad \downarrow & & \uparrow \\ & (4d_{5/2})^5(\mathrm{VB\text{-}5f})^2(\mathrm{CB\text{-}5f})^2 & \end{array} \quad (3a)$$

$$\mathrm{hv}^{\mathrm{RIPES}} = \mathrm{hv}^{\mathrm{XES}} \approx \mathrm{KE}^{\mathrm{RIPES}} \approx \mathrm{BE}\ (4d_{5/2}) \quad (3b)$$

Now, let us consider the RIPES satellite.

As the kinetic energy of the incoming electron approaches the photon energy of the satellite, another resonance is observed. It is known that RIPES is a threshold phenomenon [18,26]. Although transitions into the U6d states for direct IPES will be very weak, based upon

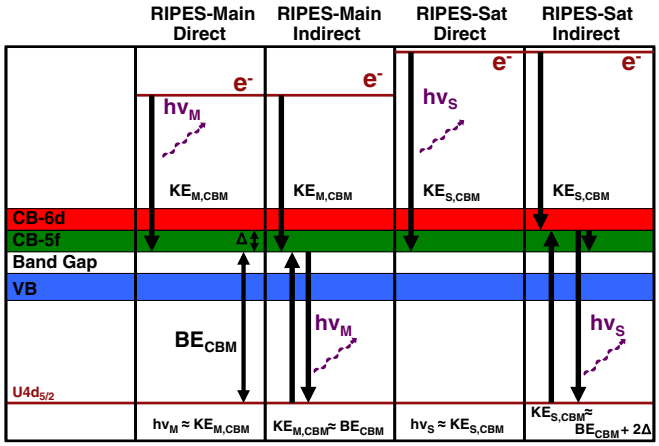

FIG. 3 (color online). A schematic of the RIPES process for the main (M) and satellite (S) peaks. hv is the energy of the outgoing photon. KE is the kinetic energy of the incoming electron. Δ is the energy (ε) separation of the U5f and U6d states in the conduction band (CB). VB is the valence band.

cross-section arguments, indirect transitions through the U6d states will be allowed. This is because the excitation step in the indirect channel is like XES, with a Coulombic matrix element and relaxed selection rules. These processes are illustrated in the right panels of Fig. 3 and shown below in Eq. (4). Here, the subscript S is used to denote the satellite.

$$\text{Direct}$$

$$e(KE_S^{RIPES}) + (4d_{5/2})^6(\text{VB-5f})^2 \rightarrow (4d_{5/2})^6(\text{VB-5f})^2(\text{CB-5f})^1 + h\nu_S^{RIPES}$$

$$\text{Indirect} \quad \downarrow \qquad \uparrow \text{2e transition} \tag{4a}$$

$$(4d_{5/2})^5(\text{VB-5f})^2(\text{CB-6d})^2$$

$$h\nu_S^{RIPES} = h\nu_S^{XES} \approx KE_S^{RIPES} \approx BE\,(4d_{5/2}) + 2\Delta \tag{4b}$$

$$\Delta = \varepsilon(\text{CB-6d}) - \varepsilon(\text{CB-5f}) \approx 7\ \text{eV} \tag{4c}$$

Δ is the energy (ε) difference between the U5f and U6d manifolds in the UDOS. This is on the scale of about 7 eV, as seen in Fig. 2. The decay step in the indirect channel is a two-electron process, with two U6d electrons dropping into the CB $-$ 5f and the U4$d_{5/2}$ core hole, with the emission of a photon. Using a model philosophically derived from that developed for multielectronic photoemission [21,22], this transition is electric dipole, with energy and momentum conservation, but divided across two electrons. The set of possible two-electron states available from two single d states have a variety of possible electric dipole transitions into the set of possible two-electron states available from a single f state and a single d state. It is crucial that the final configuration is $(4d_{5/2})^6(\text{VB} - 5f)^2(\text{CB} - 5f)^1$, consistent with the direct channel. (The result of this model has interesting implications for the true nature of the XES features, including some significant insights into the nature of shielding. However, these require some detailed discussions that will be made in a future publication.) In a sense, we have chosen to use the simplest possible model for multielectronic transitions in RIPES. We believe that this simple physical picture has given us a significant insight into the nature of RIPES and the UDOS in UO_2. Nevertheless, it would be of great use to have the as yet undeveloped RIPES variants of more sophisticated models [30,31] be applied to the analysis of our results, quantifying the possibilities of alternate spectroscopic pathways and selection rules and testing the validity of our simple model.

The salient result here is that without the need to resort to soft x-ray synchrotron radiation, it is possible to directly isolate the 5f and 6d components of the UDOS of an actinide. While nonresonant IPES will effectively sample only the 5f states, RIPES can isolate the different contributions via the separate observations of the main and satellite resonant peaks.

We have used resonant inverse photoelectron spectroscopy and x-ray emission spectroscopy, plus an accurate picture of the unoccupied density of states in uranium dioxide, to demonstrate that the 5f and 6d components of the unoccupied density of states of an actinide material can be isolated using RIPES. This bodes well for its application to the enigmatic and highly radioactive case of plutonium, where the nature of its electronic structure and the underlying electron correlation remain unknown [32,33].

Lawrence Livermore National Laboratory is operated by Lawrence Livermore National Security, LLC, for the U.S. Department of Energy, National Nuclear Security Administration under Contract No. DE-AC52-07NA27344. This work was supported by the DOE Office of Science, Office of Basic Energy Science, Division of Materials Science and Engineering. We would like to thank Wigbert Siekhaus for providing the uranium sample.

*Corresponding author
Tobin1@LLNL.Gov

[1] Y. Guerin, G. S. Was, and S. J. Zinkle, MRS Bull. **34**, 10 (2009).
[2] F. Gupta, A. Pasturel and G. Brillant, Phys. Rev. B **81**, 014110 (2010).
[3] J. R. Naegele, in *Electronic Structure of Solids: Photoemission Spectra and Related Data,* , edited by A Goldmann, Landolt-Bornstein, Numerical Data and Functional Relationships in Science and Technology, Group III, Vol. 23b, (Springer-Verlag, Berlin, 1994), pp. 183–327; and references therein.
[4] B. W. Veal and D. J. Lam, Phys. Rev. B **10**, 4902 (1974).
[5] Y. Baer and J. Schoenes, Solid State Commun. **33**, 885 (1980).
[6] G. C. Allen, I. R. Trickle, and P. M. Tucker, Philos. Mag. B **43**, 689 (1981).
[7] W. McLean *et al.*, Phys. Rev. B **25**, 8 (1982).

[8] H. R. Moser *et al.*, Phys. Rev. B **29**, 2947 (1984).
[9] H. Idriss, Surf. Sci. Rep. **65**, 67 (2010). review
[10] S. W. Yu and J. G. Tobin, J. Vac. Sci. Technol. A **29**, 021008 (2011).
[11] G. Chauvet and R. Baptist, Solid State Commun. **43**, 793 (1982).
[12] P. Roussel, P. Morrall, and S. J. Tull, J. Nucl. Mater. **385**, 53 (2009).
[13] G. Kalkowski *et al.*, Phys. Rev. B **35**, 2667 (1987).
[14] F. Jollet *et al.*, J. Phys. Condens. Matter **9**, 9393 (1997).
[15] M. Magnuson *et al.*, Appl. Surf. Sci. **252**, 5615 (2006).
[16] S.-W. Yu *et al.*, Phys. Rev. B **83**, 165102 (2011).
[17] L. E. Cox *et al.*, Phys. Rev. B **31**, 2467 (1985).
[18] M. Grioni *et al.*, J. Electron Spectrosc. Relat. Phenom. **101–103**, 713 (1999).
[19] L. Petit *et al.*, Phys. Rev. B **81**, 045108 (2010).
[20] I. D. Prodan, G. E. Scuseria, and R. L. Martin, Phys. Rev. B **76**, 033101 (2007)
[21] D. A. Shirley, in *Photoemission in Solids*, edited by M. Cardona and L. Ley (Springer-Verlag, Berlin, 1979).
[22] S. T. Manson, Adv. Electron. Electron Phys. **44**, 1 (1978); **41**, 73 (1976).
[23] T. A. Carlson, Phys. Rev. **156**, 142 (1967).
[24] D. P. Spears, H. J. Fischbeck, and T. A. Carlson, Phys. Rev. A **9**, 1603 (1974).
[25] H. Hotop and D. Mahr, J. Phys. B **8**, L301 (1975).
[26] J. G. Tobin *et al.*, Phys. Rev. B **83**, 085104 (2011).
[27] S. R. Mishra *et al.*, Phys. Rev. Lett. **81**, 1306 (1998).
[28] S.-W. Yu, J. G. Tobin, and B. W. Chung, Rev. Sci. Instrum. **82**, 093903 (2011).
[29] J. J. Yeh and I. Lindau, At. Data Nucl. Data Tables **32**, 1 (1985).
[30] G. van der Laan and B. T. Thole, Phys. Rev. B **53**, 14458 (1996).
[31] F. de Groot, Chem. Rev. **101**, 1779 (2001).
[32] J. H. Shim, K. Haule, and G. Kotliar, Nature (London) **446**, 513 (2007).
[33] S. W. Yu, J. G. Tobin, and P. Söderlind, J. Phys. Condens. Matter **20**, 422202 (2008).